

Cracks width-corrosion rate correlation on the durability of reinforced concrete in a very high aggressiveness tropical marine environment

O. Troconis de Rincón^{1*} , V. Milano¹ , A. A. Torres-Acosta² , Y. Hernández-López¹ 

*Contact author: oladistr@gmail.com

DOI: <http://dx.doi.org/10.21041/ra.v8i3.321>

Reception: 12/06/2018 | Acceptance: 02/08/2018 | Publication: 31/08/2018

ABSTRACT

The aim of this investigation was to evaluate the correlation between crack width and apparent corrosion rate in reinforced concrete specimens exposed for more than six years to a tropical marine environment, at the natural test site La Voz, Venezuela. Six specimens from DURACON Project (prismatic 15x15x60 cm, with 0.65 w/c ratio) were monitored; each specimen having six reinforcing steel bars placed at three different depths (two each at 15, 20, and 30 mm) for electrochemical tests (corrosion potential and corrosion rate). An empirical correlation between surface crack propagation rate and i_{CORR} was established, which may help i_{CORR} estimation indirectly if values of maximum surface crack widths due to reinforcement corrosion are obtained in at least one-year period of monitoring.

Keywords: reinforced concrete; marine environment; corrosion rate; cracks width.

Cite as: O. Troconis de Rincón, V. Milano, A. A. Torres-Acosta, Y. Hernández-López (2018), “Cracks width-corrosion rate correlation on the durability of reinforced concrete in a very high aggressiveness tropical marine environment”, Revista ALCONPAT, 8 (3), pp. 317-332, DOI: <http://dx.doi.org/10.21041/ra.v8i3.321>

¹ Centro de Estudios de Corrosión (CEC), Facultad de Ingeniería, Universidad del Zulia, Maracaibo, Venezuela.

² Universidad Marista de Querétaro (UMQ), Facultad de Ingeniería, Laboratorio de Materiales de Construcción; Instituto Mexicano del Transporte (IMT), Coordinación de Ingeniería Vehicular e Integridad Estructural, Sanfandila, Querétaro, México.

Legal Information

Revista ALCONPAT is a quarterly publication by the Asociación Latinoamericana de Control de Calidad, Patología y Recuperación de la Construcción, Internacional, A.C., Km. 6 antigua carretera a Progreso, Mérida, Yucatán, 97310, Tel.5219997385893, alconpat.int@gmail.com, Website: www.alconpat.org

Responsible editor: Pedro Castro Borges, Ph.D. Reservation of rights for exclusive use No.04-2013-011717330300-203, and ISSN 2007-6835, both granted by the Instituto Nacional de Derecho de Autor. Responsible for the last update of this issue, Informatics Unit ALCONPAT, Elizabeth Sabido Maldonado, Km. 6, antigua carretera a Progreso, Mérida, Yucatán, C.P. 97310.

The views of the authors do not necessarily reflect the position of the editor.

The total or partial reproduction of the contents and images of the publication is strictly prohibited without the previous authorization of ALCONPAT Internacional A.C.

Any dispute, including the replies of the authors, will be published in the second issue of 2019 provided that the information is received before the closing of the first issue of 2019.

Correlación entre ancho de grietas y velocidad de corrosión en la durabilidad de concreto reforzado en un ambiente marino tropical altamente agresivo

RESUMEN

El objetivo de esta investigación fue evaluar la correlación entre ancho de grieta producido por corrosión y la velocidad de corrosión aparente (i_{CORR}) de especímenes de concreto reforzado, expuestos por más de 6 años a un ambiente marino tropical en la estación La Voz, Venezuela. Seis especímenes del Proyecto DURACON (prismas de 15x15x60 cm, y concreto con relación a/c de 0.65) fueron monitoreados; los cuales tienen 6 varillas de refuerzo a diferentes profundidades (dos a 15, 20 y 30 mm), para las pruebas electroquímicas. Se estableció una correlación empírica entre la velocidad de propagación de la grieta superficial e i_{CORR} , que podría ayudar a estimar el valor de i_{CORR} , si se dispone de valores promedio de ancho máximo de grieta del elemento corroyéndose durante un periodo de monitoreo por lo menos de un año.

Palabras clave: concreto reforzado; ambiente marino; velocidad de corrosión; ancho de grieta.

Correlação entre a largura da fissura e a taxa de corrosão na durabilidade do concreto armado em um ambiente marinho tropical altamente agressivo.

RESUMO

O objetivo desta investigação foi avaliar a correlação entre largura de fissura e taxa de corrosão aparente em espécimes de concreto armado expostos há mais de seis anos a um ambiente marinho tropical, no local de teste natural La Voz, Venezuela. Seis espécimes do Projeto DURACON (15x15x60 cm prismáticos, com relação 0,65 w / c) foram monitorados; cada espécime possui seis barras de aço de reforço colocadas em três profundidades diferentes (duas de 15, 20 e 30 mm cada) para testes eletroquímicos (potencial de corrosão e taxa de corrosão). Uma correlação empírica entre taxa de propagação de trincas superficiais e i_{CORR} foi estabelecida, o que pode ajudar a estimar a i_{CORR} indiretamente se valores de largura máxima de trincas superficiais devido à corrosão de reforço forem obtidos em pelo menos um ano de monitoramento.

Palavras-chave: concreto reforçado; ambiente marino; velocidade de corrosão; ancho de grieta.

1. INTRODUCTION

During the last 20 years, the term concrete durability has been used more frequently among members of the scientific society worldwide. In some developed countries as the United States of America, Spain, France, United Kingdom, and Japan, durability has been addressed as a very important subject, attracting seven figures investment for research in this area. Reinforced concrete structure deterioration due to rebar corrosion has increased as consequence of cracks on the concrete cover surface. Many investigations so far, have been performed based on the study of durability during the initiation period. However, very few have been focused toward its performance during its residual life.

Some studies related to the residual life stage of concrete structures, have been made where accelerated corrosion was performed by applying a constant anodic current to the rebars (Tachibana, et.al., 1990; Huang and Yang, 1997; Rodriguez et.al., 1997; Almusallam, et.al., (1997); Cabrera, 1996). After applying such anodic currents to the rebar in a short period of time, reduction of the structural capacity was correlated with corrosion parameters such as gravimetric metal loss and corrosion-induced concrete cracking (Almusallam, 1997; Mangat and Elgarf, 1999; Torres-Acosta, 1999). Torres-Acosta, 1999; Torres-Acosta and Martínez-Madrid, 2003, have conducted several studies related to

this subject, but also under natural conditions (Torres-Acosta and Castro-Borges, 2013; Cabrera-Madrid et al, 2014). In a previous investigation (Torres-Acosta and Martínez-Madrid, 2003), they reported results on residual life degradation parameters, using reinforced concrete slabs (0.42 w/c ratio, chloride contamination during mixing to accelerate rebar corrosion) and no anodic current application. At the end of the experimentation, corrosion-induced crack position, width, and length were measured and correlations with the cross-section mass loss were also performed. Based in their experimental results, empirical relationships between average rebar radius loss (x_{AVG}) divided by the original rebar radius (r_0) and load capacity were established. As an example, 10% radius loss might result in a 50% load capacity loss in reinforced concrete beam elements. They also developed an empirical relationship between crack width, WC, and the relation x_{AVG}/r_0 . Apparently, when corrosion rate is small ($12-60 \mu\text{m y}^{-1}$) cracks appear and grow in length and width faster than in accelerated corrosion tests. Finally, the last empirical correlation obtained included x_{AVG} and maximum pit depth (PIT_{MAX}), giving a factor of seven times: $PIT_{MAX} \sim 7 \cdot x_{AVG}$ (Torres-Acosta and Martínez-Madrid, 2003).

Subsequently, in 2003, Vidal et.al. studied crack width and rebar diameter loss due to corrosion in reinforced concrete beams (0.5 w/c, 35 g l^{-1} NaCl contamination). They discussed that reinforcement corrosion obtained in this investigation is closer to what is observed in natural conditions (with respect to the distribution of corrosion, types of corrosion, and oxides produced) than the obtained by impressed current or addition of calcium chloride in concrete. They developed a new model relating crack width vs. rebar cross section loss and observed that the rebar cross section loss seems to be independent of their diameter and the concrete cover/rebar diameter ratio, except when evaluated in the period of crack initiation.

In 2007, Torres-Acosta et.al. reported an empirical correlation between rebar corrosion rate and crack width, using reinforced concrete beams (0.6 w/c, contaminated with NaCl: 1 wt% Cl^- on cement basis), and subjected to a bending stress. The beams were sprayed in a central area of 25 cm long twice a week, with saline solution (3.5 wt% Cl^-) in order to accelerate rebar corrosion in this area. They concluded that in a process of natural corrosion, cracks generated by the corrosion products expansion develop more slowly (width and length) than those generated by accelerated corrosion. The results obtained, showed that for a corrosion radius loss (x_{AVG}/r_0) from 4% to 10%, cracks were produced with a maximum width (CW_{MAX}) of 0.1 mm and 1 mm, respectively. The trend obtained in this study was similar to that obtained in previous research with natural corrosion (Torres-Acosta and Castro-Borges, 2013; Cabrera-Madrid et al, 2014).

The present work show the results of one of DURACON project test natural exposure sites (La Voz, Venezuela). It was located in a coastal marine environment of high aggressiveness, where some of the reinforced concrete prisms (0.65 w/c ratio concrete) in this project presented surface corrosion-induced cracks, and an empirical correlation was obtained between maximum cracks width and corrosion rate (i_{CORR}) expressed as average rebar radius loss (x_{AVG}/r_0) from natural corrosion data.

2. EXPERIMENTAL PROCEDURE

2.1 Prismatic specimens

In this investigation, reinforced concrete prismatic specimens from DURACON project (Troconis de Rincón et.al., 2007) were used. These were installed in a project's natural exposure sites called La Voz (in Venezuela), classified as marine environment of very high aggressiveness (>C5 according to ISO⁽¹⁾ 9223: 2012. Figure 1 shows a schematic diagram of the prismatic specimens under evaluation. Concrete prisms of 15x15x30 cm (0.65 w/c ratio) and reinforced with six rebars

⁽¹⁾ISO, 1, Ch. de la Voie-Creuse, Case postale 56, CH-1211 Geneva 20, Switzerland.

(9.5 mm in diameter), placed at different concrete depths (two each at 15, 20 and 30 mm). Three of them were placed at the windward face and the other three on the leeward face. The ends of each bar were protected with epoxy coating to avoid oxygen differential and crevice corrosion, leaving a central portion of 15 cm length uncovered. Figure 2 shows the specimen supports installed at La Voz test station.

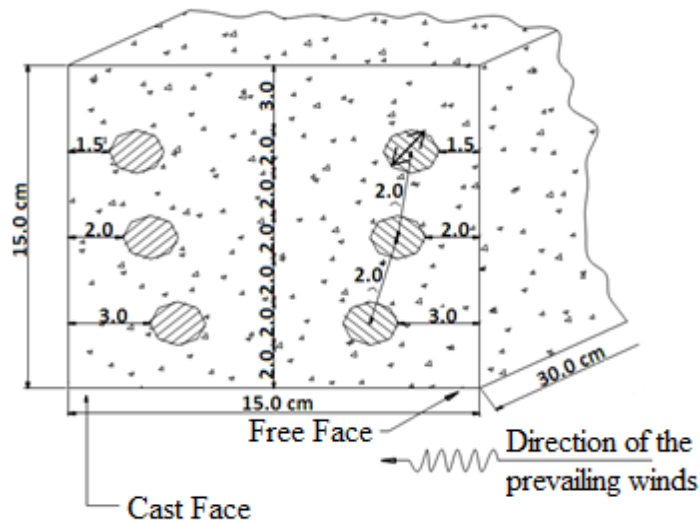


Figure 1. Schematic diagram of the rebar configuration in the concrete specimen



Figure 2. Test Station in Marine Environment (La Voz)

2.2 Environmental assessment

Climatic and environmental parameters were assessed according to the methodology established by ISO 9223 standard determining environmental aggressivity in the test station. Parameters as relative humidity (RH), time of wetness (TOW/ τ), wind speed and direction, rainfall amount, daily temperature, chloride concentration, CO₂ concentration and sulfur compounds concentration, were measured during the experimental period. It is important to mention that there are currently no regulations to identify the aggressiveness of the environment for reinforced concrete structures; therefore, ISO standard for metallic materials was used as a first approach.

2.3 Electrochemical evaluation

For electrochemical monitoring, a GECOR 6^(†2) field corrosimeter instrument was used, which measured corrosion potential (E_{CORR} , vs. Cu/CuSO₄ reference electrode), and corrosion rate (i_{CORR}) of the reinforcement, by the linear polarization technique (Feliú et.al., 1993).

2.4 Cracks survey

Rebar corrosion-induced concrete surface cracks, both in the windward face as well as in the leeward face were monitored by a careful visual examination using a (nonstandard) 15cm x 30cm grid to report the length and location of each corrosion crack. Cracks widths were measured using a crack comparator card. Thereby, an overview crack map was recorded, showing the length, location, and width of all cracks in all specimens. Experimental data were fitted linearly and compared with data obtained by other authors with natural and accelerated corrosion techniques. In order to assess the rebar cross section loss, an estimate was made using the area under i_{CORR} vs. time plot. This value was then correlated with maximum crack width (MCW), corresponding to each of the rebars of the specimens tested. Rebar mass loss estimates were calculated using Faraday law (Equation [1]):

$$\Delta W_f = \frac{55.5}{n \times F} \left(\int I dt \right) \quad (1)$$

Where: ΔW_f is faradaic mass loss (g); 55.85 g/mol is the atomic weight of Fe; $\int I dt$ is the area under the curve i_{CORR} vs. time; n is the valence number for iron (+2), and F is Faraday's constant (96,500 C/mol). This value is then used to estimate the average radius loss due to corrosion (X_{AVG}), in mm, which is calculated using Equation (2):

$$X_{avg} = \frac{\Delta W_f \times 1000}{\rho \times \pi \times D \times l} \quad (2)$$

Where: ρ , iron density (gr/cm³); D , rebar diameter (mm) and l , length of the rebar (mm). At the end of the experimentation, concrete specimens were demolished and the steel rebars were retrieved to determine the real cross section loss based on average pit depth estimates.

3. RESULTS AND DISCUSSION

3.1 Environmental assessment

Figure 3 shows the weather parameters results of the natural test site monitored during the exposure time. It is clear to observe the rain-drought periods, typical of tropical environments. There was only one short period of high rain precipitation and was at the end of year 2006, as a result of the weather phenomenon caused by hurricane Ivan, which passed through the Lesser Antilles and the Caribbean Sea.

Regarding monthly average temperature, it varied only 3 °C during the entire evaluation period (six years). The minimum value was 26.7 °C (March 2003 and February 2009), while the maximum value was about 30 °C (October 2004 and September 2008). The small variations observed for this parameter, shows a climatic stability in this test station and the geographic region itself.

^(†2) Trade name

The highest monthly average relative humidity (RH) value from the whole evaluation period was observed in August 2004, which was 84%. This coincides with the highest rain precipitation value for the year.

For wind speed data, in general it can be seen that it vary in a range between 17 and 24 km/h, with large variations when sudden changes occur in the microclimate, as the phenomena that have been explained above where the wind speed was substantially increased. Chloride and sulfate estimates present in this atmosphere and the time of wetness during the 6-year exposure time are shown in Table 1. A very high corrosive ambient, according to ISO 9223, for the first three years of this test station, was corroborated based on the monitoring of parameters in Table 1. For the 4th and 5th year, a decrease in corrosivity was noticed, possibly due to high rainfall from storms and hurricanes occurred in those years; however, remains highly corrosive. The time of wetness (TOW) was also estimated with the weather parameters such as temperature and RH using ISO procedure (see Table 1).

Table 1. Aggressive agents and time of wetness (TOW) at the test station La Voz

Evaluation Time (y)	Chlorides (mg m ⁻² d ⁻¹) /S		Sulfates (mg m ⁻² d ⁻¹) /P		TOW (hy ⁻¹) /τ		ISO 9223 Corrosivity class
1	683.907	S3	22.645	P1	4818	τ4	C5
2	382.561	S3	27.800	P1	4818	τ4	C5
3	128.898	S2	19.726	P1	6132	τ5	C5
4	154.159	S2	13.111	P1	3451	τ4	C4
5	165.691	S2	5.616	P0	2823	τ4	C4
6	183.682	S2	-		-		-

Corrosion induced by chloride ions attack was favored because high relative humidity facilitates the transport of aggressive agents in the atmosphere enhanced by the high temperature, which accelerates localized corrosion of the bars.

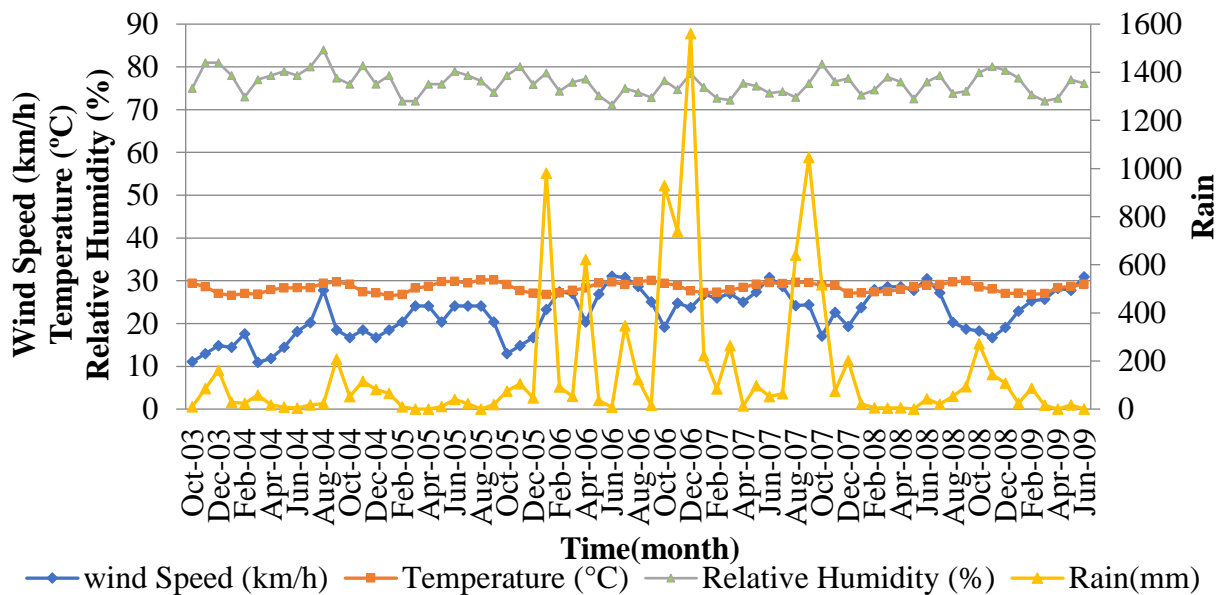


Figure 3. Behavior of meteorological parameters at test station La Voz.

3.2 Electrochemical parameters

Figures 4 and 5 show the results obtained from the electrochemical monitoring: corrosion potential and corrosion rate vs. time for 15-mm and 30-mm concrete depth rebar, respectively. These figures clearly show the time in which the bars began to depassivate (E_{CORR} and i_{CORR} more negative than -250 mV vs. Cu/CuSO₄ and greater than 0.1 $\mu\text{A}/\text{cm}^2$, respectively); coinciding with the first change in slope of the accumulated corrosion rate vs. time curve. In addition, these figures show 30-mm depth rebars stayed passive for longer time than the 15-mm depth rebars, but the propagation rate for the first set were higher than the second set. This might be due to the winds at the La Voz natural test site did not show a preferential trade wind direction (North-East in this case), but rather slashing winds which also allows the ingress and diffusion of chloride ions through the prism's bottom face. This was the top cast face and the most porous one, which was the closer to the deeper bars (30-mm depth rebars), thus giving this unusual performance.

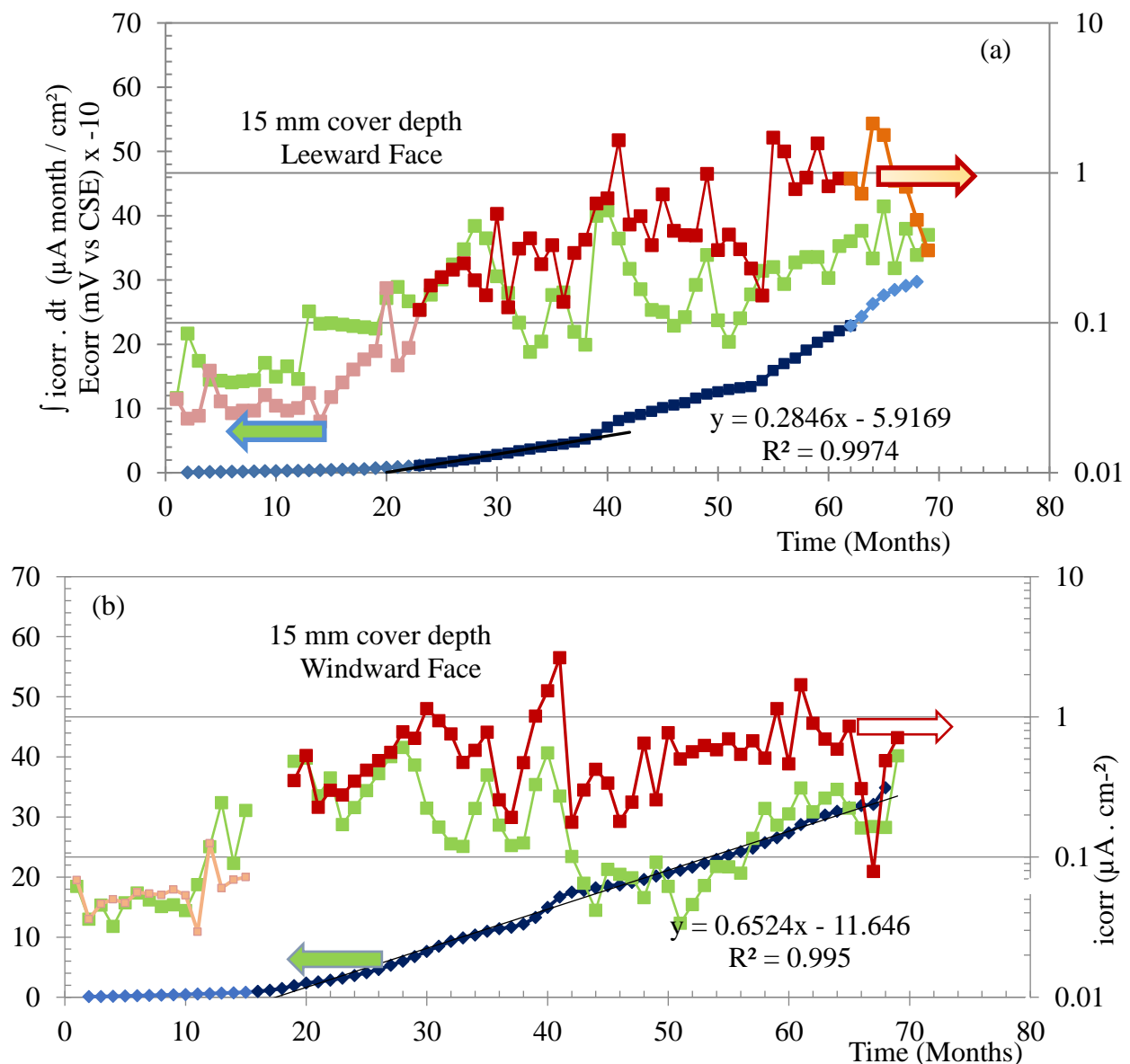


Figure 4. Electrochemical parameter monitoring (E_{CORR} ; i_{CORR} and cumulative i_{CORR} values) vs. time for 15-mm concrete depth rebar, leeward (a) and windward (b) faces.

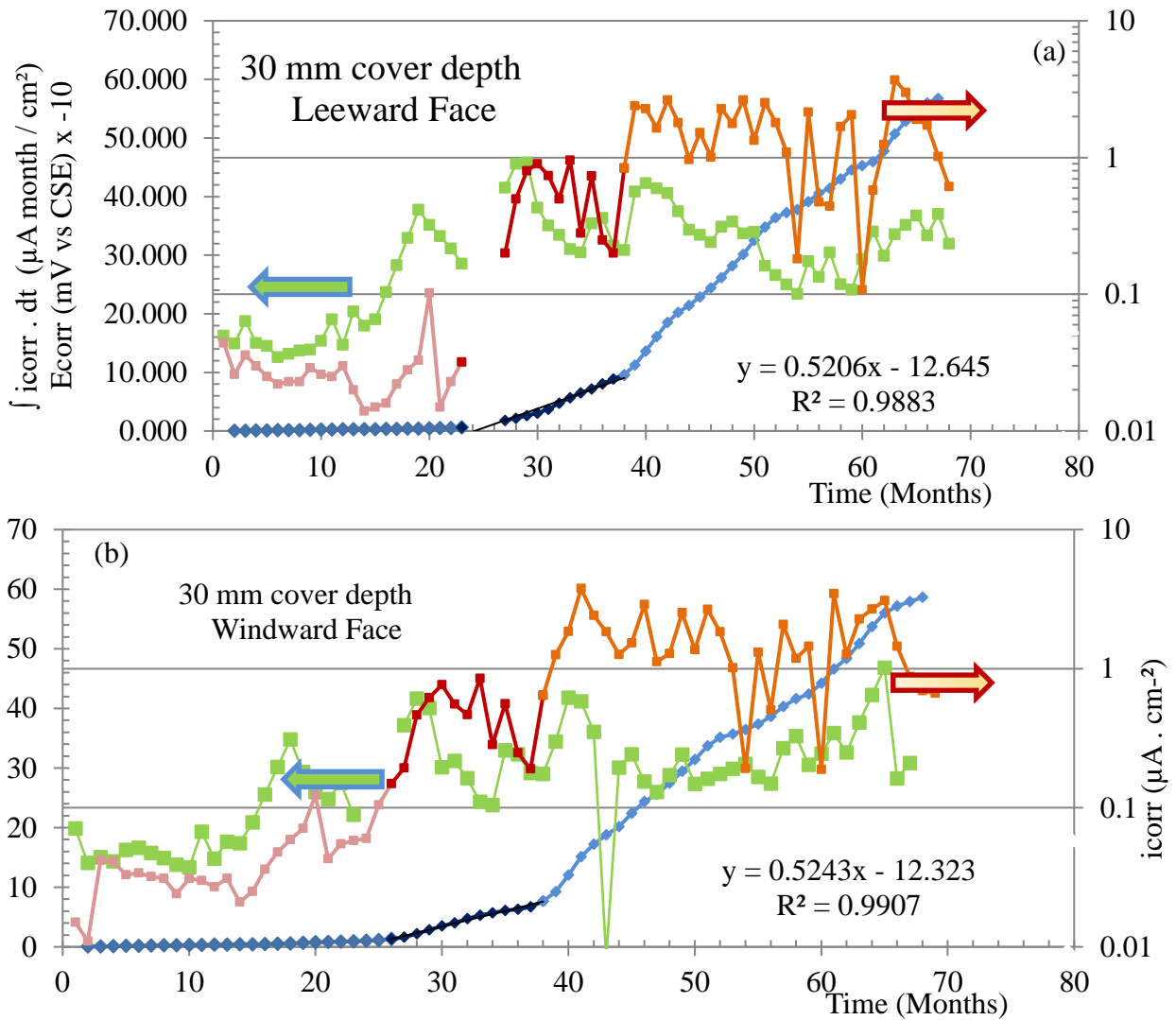


Figure 5. Electrochemical parameter monitoring (E_{CORR} ; i_{CORR} and cumulative i_{CORR} values) vs. time for 30-mm concrete depth rebar, leeward (a) and windward (b) faces.

3.3 Crack width and corrosion rate correlation

Figure 6 shows the state in which one of the three representative specimens were found after a 6 year exposure period in La Voz natural test site. This figure also shows a photograph of the specimen's windward face and a schematic representation of the surface fissures/cracks survey that presented such specimen.

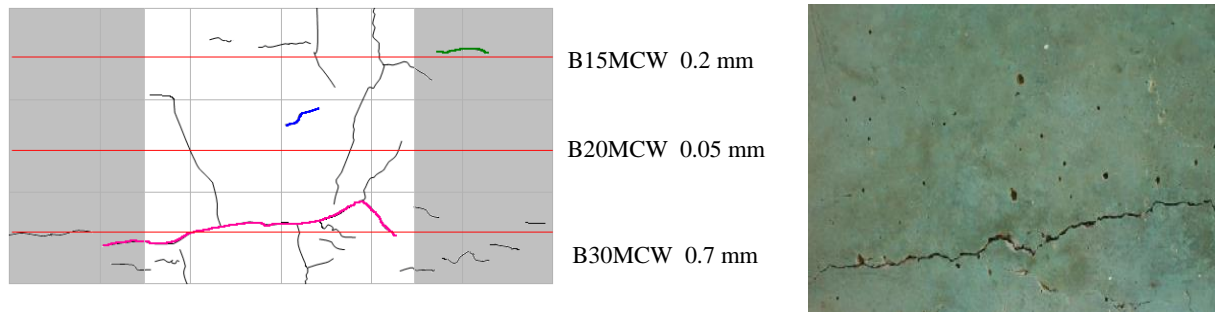


Figure 6. Specimen 6 (w/c ratio 0.65, and windward face) surface crack survey (left) and photographic evidence of such distress (right)

Figure 7 shows that with increasing loss of cross section area of the rebars (estimated from $\int i_{CORR}dt$ data and equations 1 and 2), the surface MCW also increases (at the specimen's windward face). The effect of the concrete cover on crack initiation and propagation (on the windward face) was also demonstrated in Figure 7: crack widths were bigger at rebars with smaller concrete cover having the same rebar cross section loss. This might be due to the concurrent effect of high relative humidity prevailing in the area (> 80%) together with a high chloride ions content, which maintains moisture inside the bulk concrete, such that the chloride ions (129-684 mg m⁻²d) can diffuse easily, promoting reinforcement corrosion.

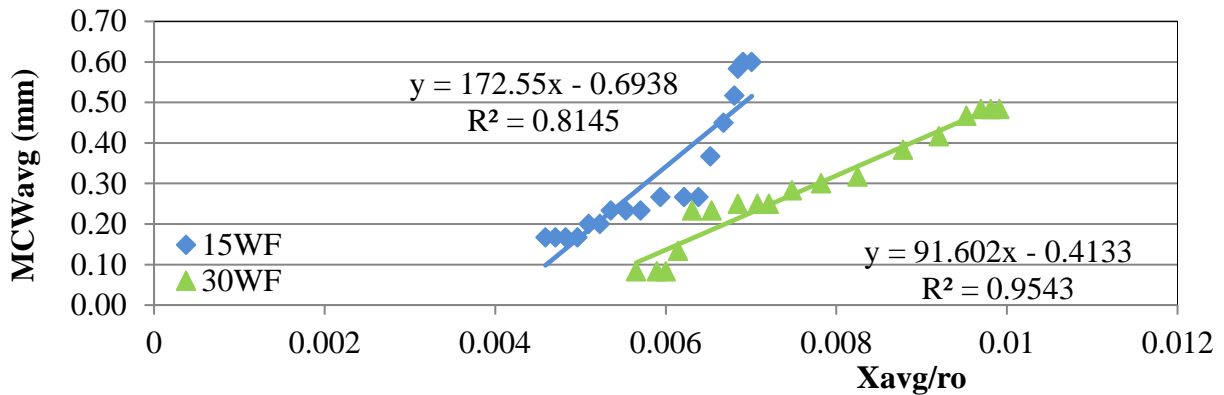


Figure 7. Average maximum crack width of concrete in relation to the rebar cross section loss, at the natural test site La Voz, w/c ratio 0.65, windward face

It is also important to mention that there is a direct relationship between the MCW and rebar's x_{AVG}/r_0 . The goodness of the correlation is high for the first years of exposure (MCW < 0.3 mm), while for MCW's wider than 0.3 mm the data was disperse, causing the correlation to decrease. Additionally, the mean MCW increases with very little loss of material due to corrosion. Also when MCW's are too wide, voids were created, which interfered with the i_{CORR} measurement using the described corrosimeter field instrument. This raises some doubts over the last year's i_{CORR} data, which was used to obtain x_{AVG}/r_0 . Thus, it was necessary to discard the latest i_{CORR} measurements and determine the correlation between MCW and x_{AVG}/r_0 using first year data.

A more representative correlation between MCW and x_{AVG}/r_0 are presented in Figure 8, where the last years i_{CORR} bias measurements of both bars were removed, thus better correlations were obtained ($R^2 \sim 0.9722$ and 0.9038 for 15-mm and 30-mm depth rebar, respectively).

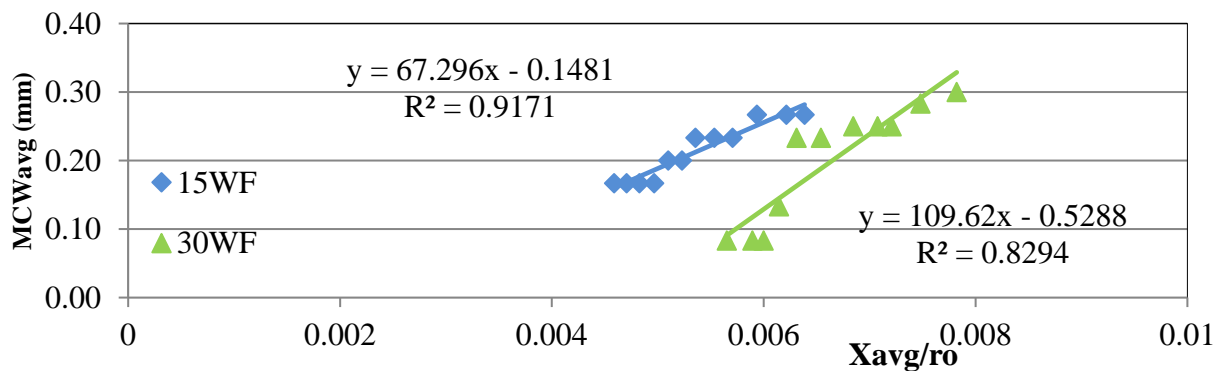


Figure 8. Representative behavior (last year's data removed) of the average maximum crack width of concrete in relation to the rebar cross section loss, at the natural test site La Voz, w/c ratio 0.65, windward face

Figure 9 shows a typical crack surveys and photograph of one of the specimen's leeward face from a representative 0.65 w/c concrete specimen after 6 years of exposure. As observed from these results, wider cracks were observed than at the windward face. This performance might be due because it remains wet for longer periods of time, which favors the transport of characteristic environment's aggressive agents, and spread into the bulk concrete as compared to the windward face, which was in continuous contact with hot/high speed wind that could dry out the concrete's internal moisture. This performance is observed also in Figures 4 and 5, where the corrosion rates of leeward face rebars show small increments at the end of the exposure period.

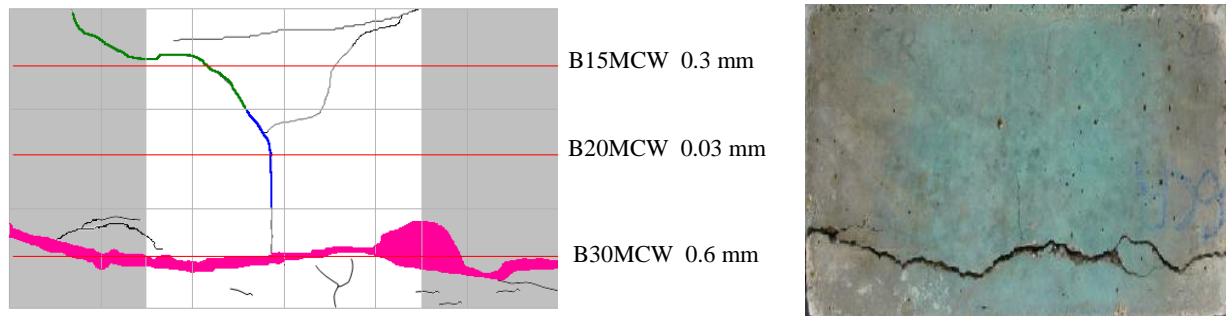


Figure 9. Left, General map of cracks and right, photo of the specimen 6, w/c ratio 0.65, leeward face

Similarly to the windward face data, the leeward face data did not have good correlation between the MCW and rebar's x_{AVG}/r_0 when cracks were wider than 0.5 mm, and the last year data points were also bias. Thus in Figure 10, the more representative relationship between MCW and x_{AVG}/r_0 was obtained by removing last year's data of the two rebars, which significantly improves the correlation ($R^2 \sim 0.9397$ and 0.9843 for the 15-mm and 30-mm depth rebar, respectively).

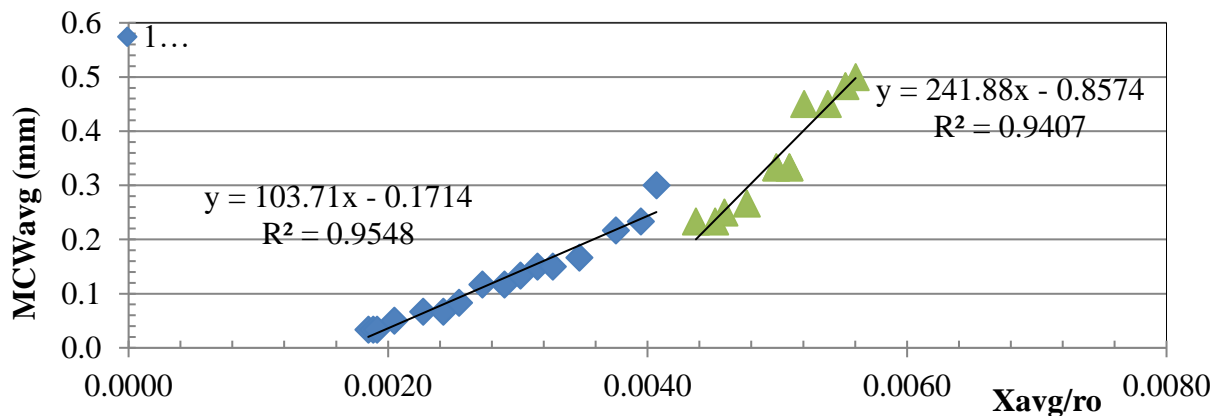


Figure 10. Representative behavior (last year's data removed) of the average maximum crack width in relation to the loss cross section area of the bar at the test station La Voz, w/c ratio 0.65, leeward face

On the other hand, the effect of concrete cover on crack propagation unexpectedly was the opposite than the windward performance: the largest crack widths were found for the 30-mm depth rebar. This might be due to (as explained in Section 3.2) the winds at the La Voz natural test site did not show a preferential trade wind direction (North-East in this case), but rather slashing winds which also allows the ingress and diffusion of chloride ions through the prism's bottom face. This was the top cast face and the most porous one and the closer to the deeper bars (30-mm depth rebar), thus giving this unusual performance.

Figure 11 shows as a comparison, a compilation of the MCW_{avr} (average MCW) and x_{avr}/r_0 data obtained in this investigation together with data from a previous investigation (Torres-Acosta and Martínez-Madrid, 2003) with natural and accelerated corrosion conditions. Accelerated corrosion data was plotted in Figure 11 using symbols without any filling color, as compared the natural corrosion data symbols, which all are either black filled for previous investigations data or blue-pink-orange for this investigation data.

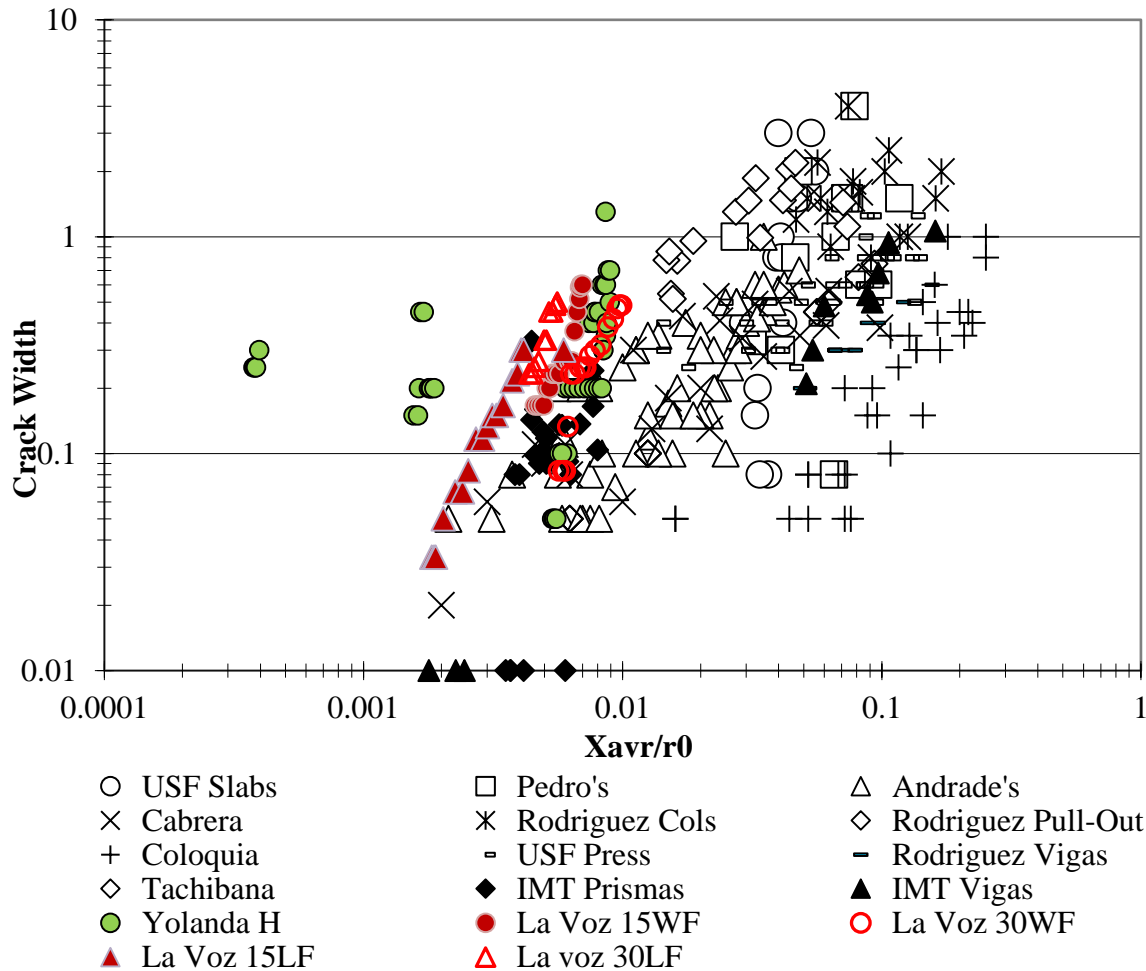


Figure 11. Data compilation of average maximum crack width in relation to the loss cross section area of the bar for different authors and test conditions (Torres-Acosta and Martínez-Madrid, 2003)

It is observed that in the case of accelerated corrosion methods, data follow a good trend and are close from each other (Torres-Acosta and Martínez-Madrid, 2003). There is also a difference between accelerated corrosion data from reinforced concrete (Δ , \times , \diamond , \circ , \times , \square symbols) vs prestressed concrete (+ symbol) elements when general corrosion was obtained: wider cracks were observed from reinforced concrete elements than from prestressed concrete elements. If the corrosion is localized in a small area of the strand (- symbol) in prestressed concrete elements instead of general corrosion (+ symbol), the crack widths trend was similar than the obtained in reinforced concrete elements. Therefore, if the entire prestressed strand (or wire) is corroded, the crack propagation apparently was mitigated by the compressive state of stresses in the concrete, but if the prestressed strand (or wire) corrodes only in a short portion of the entire length, the crack propagation follows reinforced concrete elements trend.

On the other hand, natural corrosion data presented a more disperse performance than accelerated corrosion, as seen from the colored symbols. In general, the natural corrosion data follows similar trend than accelerated corrosion data, but with higher crack widening (higher Crack Width vs x/r_0 slope). The higher crack propagation rate in natural corrosion tests may indicate that crack repair might be done earlier than the obtained from accelerated corrosion tests. This performance must be checked with collection of a larger data from the literature and data in the remaining DURACON project outcomes.

Data from this investigation follows a well-defined trend: less corrosion-induced material loss is required for cracks to appear at the concrete element surface. In natural conditions, like the present investigation's specimens, the concrete is affected by the ingress of aggressive agents such as chlorides ions, which produce a localized rupture of the passive film until corrosion products are formed in sufficient amount to crack the concrete, which depends on concrete quality (internal porosity).

This cracking process on low quality concrete, may requires a smaller amount of corrosion products for crack formation and propagation (Torres-Acosta and Castro-Borges, 2013; Torres-Acosta et al., 2007). But compared with previous investigations with natural corrosion specimens exposed during a period between 3 and 6 years (■, ●, ◆ symbols), there is a difference of, approximately, 10 times the amount of mass needed to produce the same crack wideness.

It is important to remind that data from this investigation were obtained from electrochemical mass loss determinations, mainly linear polarization resistance (or also known as R_p). If corrosion were uniform, the faradaic metal loss might be twice as much as the estimated gravimetric metal loss, but if rebar corrosion is localized (i.e. pitting corrosion), the faradaic metal loss could be estimated even up to ten times the gravimetric metal loss (González et.al., 1995). All rebar radius loss data in Figure 11 was estimated from gravimetric procedure, except data from Hernández et.al.2016 (green color points) and the present investigation. Actual rebar loss estimates in these two investigations also have the particularity of being performed in highly porous concrete (with w/c ratio > 0.65), therefore, lower mechanical strength and easier crack formation is also expected.

Similar concrete type was used by Hernández et.al., 2016, to fabricate beams that were some of them loaded at the same time they were exposed to chloride rinse at the center of the beam elements to produce corrosion without using anodic currents. As seen in Figure 11, data from loaded beams (Hernández et.al., 2016) separate from all the natural and accelerated data to lower radius loss for same MCW_{avr} opening. This performance might be due to not only the possible differences between gravimetric and the faradaic mass loss, but also from the applied tensile stresses from flexure loading application, that may increase the crack opening propagation rate. In same reference some other beams were unloaded, thus the MCW_{avr} vs x/r_0 data follows similar trend than the present investigation where concrete prism tested maintained unloaded during experimentation.

3.4 Empirical correlation between reinforcement corrosion rate and surface crack propagation rate

Figure 12 shows the crack width propagation vs. time of exposure. As observed in this figure, there is no correlation between rebar depth and crack propagation for these specimens located at La Voz, Venezuela, test site. Two of the cracks on each rebar depth behaved in the same range of maximum crack widths (between 0.05 and 0.3 mm), and only one of such cracks showed wider maximum crack (about 0.4 mm and above). The regression lines for each crack propagation are also shown in Figure 12, showing goodness fitness above 0.8. The slope of such regression lines are considered in this investigation as the surface crack propagation rate (SCPR in mm/month).

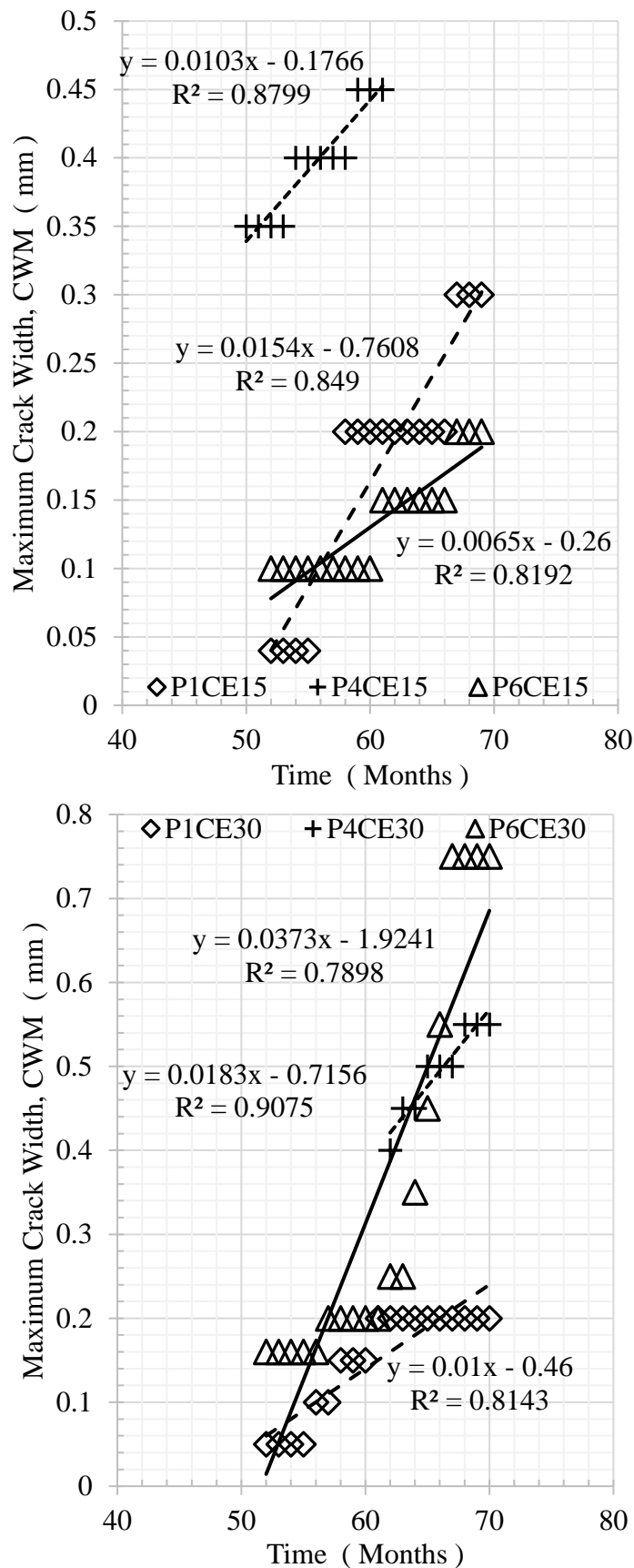


Figure 12. Crack propagation survey for w/c ratio 0.65 concrete specimen 1, windward face, La Voz, Venezuela, natural test site (a) 15 mm rebar depth and (b) 30 mm rebar depth

Based on the available data up to date, an empirical correlation between SCPR and i_{CORR} results was performed and shown in Figure 13. As observed from this figure, there is not an apparent difference between the correlation for 15 mm and 30 mm. Upon further experimental data from the other w/c ratio concrete prisms in La Voz, Venezuela, test site and the other active corrosion prisms, when surface cracks appeared at the concrete element, the rate of widening is directly proportional to the i_{CORR} of the rebar, which in turns is the expansive oxides to produce such cracks.

This empirical correlation will help to establish an indirect estimate of the corrosion rate of the reinforcing steel if the people in charge of the maintenance of the corroded structure is not able to have test equipment to determine such electrochemical values, and only a crack width survey is performed in a period of time for at least one year (12 months).

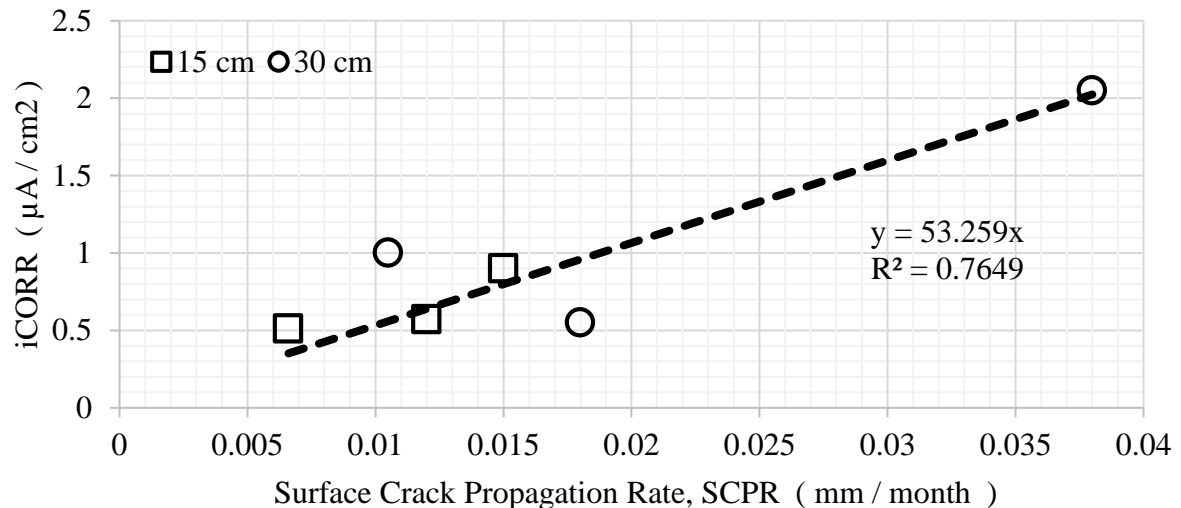


Figure 13. Empirical correlation between SCPR and i_{CORR} , 0.65 w/c ratio concrete prisms, La Voz, Venezuela, natural test site

4. CONCLUSIONS

1. An excellent correlation between average maximum crack width (MCW_{AVER}) and corrosion-induced radius loss (x_{AVG}/r_0) (rebar with 15 mm and 30 mm concrete cover, at windward and leeward faces, for 0.65 w/c ratio specimens) was found, which can be used to predict the rebar section loss for a given crack width.
2. MCW_{AVG} vs x/r_0 trend slope for natural corrosion data was higher than the obtained from accelerated corrosion data. This might reduce time for rehabilitation of corroded concrete elements in naturally exposed structures in marine environment.
3. An empirical correlation between surface crack propagation rate (SCPR) and i_{CORR} was established for 0.65 w/c ratio prisms exposed to La Voz, Venezuela, test site, which can help to estimate i_{CORR} indirectly if values of MCW_{AVR} of corroding element are obtained in a period of time of at least one year.

5. ACKNOWLEDGMENTS

The authors would like to thanks CYTED and the Universidad del Zulia for funding this research, and all people whom help with the corrosion and crack survey monitoring for such a long period of time, this would not have being possible without them; also to Dr. Douglas Linares to help in the translation of the paper.

6. REFERENCES

- Almusallam, A. A., Al-Gahtani, A. S., Maslehuddin, M., Khan, M. M., Aziz, A. R. (1997), *Evaluation of Repair Materials for Functional Improvement of Slabs and Beams with Corroded Reinforcement*. Proc. ICE-Struct. Build 122 (1): 27-34.
- Cabrera, J.G. (1996), *Deterioration of concrete due to reinforcement steel corrosion*, Cement and Concrete Composites, 18 (1), pp. 47-59. [https://doi.org/10.1016/0958-9465\(95\)00043-7](https://doi.org/10.1016/0958-9465(95)00043-7)
- Cabrera-Madrid, J. A., Balancán-Zapata, M., Torres-Acosta, A. A., Castro-Borges, P. (2014) “*Effect of tropical marine microclimates on depassivation and corrosion-induced cracking of reinforced concrete*,” International Journal of Electrochemical Science, vol. 9, pp. 8211 – 8225, ISSN: 1452-3981.
- Feliú, S., González, J. A., Feliú, V., Feliú, S. Jr., Escudero, M. L., Rodríguez Maribona, I. A., Ausin, V., Andrade, M. C., Bolano, J. A., Jimenez, F. (1933), *Corrosion detecting probes for use with a corrosion-rate meter for electrochemically determining the corrosion rate of reinforced concrete structures*, U.S., Patent 5259944 A.
- González, J. A., Andrade, C., Alonso, C., Feliú, S. (1995), *Comparison of rates of general corrosion and maximum pitting penetration on concrete embedded Steel reinforcement*. Cement and Concrete Research, 25 (2), pp. 257-264. [https://doi.org/10.1016/0008-8846\(95\)00006-2](https://doi.org/10.1016/0008-8846(95)00006-2)
- Hernández, Y., de Rincón, O., Torres, A., Delgado, S., Rodríguez, J. (2016), “*Relación entre la Velocidad de Corrosión de la Armadura y el Ancho de Fisuras en Vigas de Concreto Armado Expuestas a Ambientes que Simulan el Medio Marino*”. Revista ALCONPAT, 6 (3), pp. 272-283. DOI: <http://dx.doi.org/10.21041/ra.v6i3.152>.
- Huang, R., Yang, C. C. (1997), *Condition Assessment of Reinforced Concrete Beams Relative to Reinforcement Corrosion*. Cement and Concrete Composites, 19 (2), pp. 131-137. [https://doi.org/10.1016/S0958-9465\(96\)00050-9](https://doi.org/10.1016/S0958-9465(96)00050-9)
- ISO 9223:2012 (latest revision), “*Corrosion of metals and alloys -- Corrosivity of atmospheres -- Classification, determination and estimation*”, (Geneva, Switzerland: ISO).
- Mangat, P. S., Elgarf, M. S. (1999), “*Strength and serviceability of repaired reinforced concrete beams undergoing reinforcement corrosion*”. Magazine of Concrete Research, 51 (2), pp. 97-112. <https://doi.org/10.1680/mac.1999.51.2.97>
- Rodríguez, J., Ortega, L. M., Casal, J. (1997), *Load carrying capacity of concrete structures with corroded reinforcement*, Construction and Building Materials, 11 (4), pp. 239-248. [https://doi.org/10.1016/S0950-0618\(97\)00043-3](https://doi.org/10.1016/S0950-0618(97)00043-3)
- Tachibana, Y., Maeda, K. I., Kajikawa, Y., Kawamura, M. (1990). “*Mechanical behaviour of RC beams damaged by corrosion of reinforcement*. *Corrosion of Reinforcement in Concrete*” in Third International Symposium on Corrosion of Reinforcement in Concrete Construction, paper no. 00606810: Elsevier Science Publishers/CICC Publications, ISBN: 1-85166-487-4, May 21-24, p. 178-187.
- Torres Acosta, A.A. (1999) “*Cracking induced by localized corrosion of reinforcement in chloride contaminated concrete*”, Ph.D. Thesis, University of South Florida, Tampa, FL.
- Torres Acosta, A. A., Martínez Madrid, M. (2003), *Residual Life of Corroding Reinforced Concrete Structures in Marine Environment*. Journal of Materials in Civil Engineering, 15 (4), pp. 344-353. [https://doi.org/10.1061/\(ASCE\)0899-1561\(2003\)15:4\(344\)](https://doi.org/10.1061/(ASCE)0899-1561(2003)15:4(344))
- Torres Acosta, A. A., Hernández, Y., Troconis de Rincón, O., Delgado, S., Rodríguez, J. (2007). “*Agrietamiento de vigas de concreto por corrosión del acero de refuerzo cuando se les aplica una carga externa permanente*,” Boletín del Instituto Mexicano del Transporte (IMT), Notas 109, N°2, <http://ww.imt.mx/SitioIMT/Boletines/resumen-boletines.aspx?IdArticulo=314&IdBoletin=110> (Aug. 05, 2014).

- Torres-Acosta, A. A. and Castro-Borges, P. (2013). “*Corrosion-Induced Cracking of Concrete Elements Exposed to a Natural Marine Environment for Five Years*”, Corrosion, v. 69, No. 11, November, pp. 1122-1131, ISSN: 0010-9312.
- Troconis de Rincón, O., et al. (2007), “*Effect of the marine environment on reinforced concrete durability in Iberoamerican countries: DURACON project/CYTED*”. Corrosion Science, 49 (7), pp. 2832-2843, <https://doi.org/10.1016/j.corsci.2007.02.009>
- Vidal, T., Castel, A., Françoise, R. (2004), “*Analyzing crack width to predict corrosion in reinforced concrete*”, Cement and Concrete Research, 34 (1), pp. 165-174. [https://doi.org/10.1016/S0008-8846\(03\)00246-1](https://doi.org/10.1016/S0008-8846(03)00246-1)